

# Observations of Physical Aging in a Polycarbonate and Acrylonitrile–Butadiene–Styrene Blend

Jacky K. Y. Tang, Pearl Lee-Sullivan

Department of Mechanical and Mechatronics Engineering, University of Waterloo, Ontario N2L 3G1, Canada

Received 25 May 2007; accepted 16 April 2008

DOI 10.1002/app.28554

Published online 13 June 2008 in Wiley InterScience (www.interscience.wiley.com).

**ABSTRACT:** The effects of physical aging of a 75 : 25 PC/ABS blend have been studied using differential scanning calorimetry (DSC) and Fourier transform infrared spectroscopy (FTIR). From DSC, two distinct peak endotherms at about 90°C and 110°C, which are associated with the glass transition of ABS ( $T_{g,ABS}$ ) and PC ( $T_{g,PC}$ ) components, respectively, were observed. When progressive aging was monitored at 80°C for over 1000 h, the changes in enthalpic relaxation, glass and fictive temperatures for the blend followed similar trends to those already seen in the literature for PC aged between 125 and 130°C. The rate of enthalpy relaxation was also comparable. The plot of peak endotherm against logarithmic aging time for the PC blend constituent, however, behaved quite differently from the linear relationship known for highly aged PC. The ABS peak component also appeared to be insensitive to aging. Both observations were confirmed to be statistically significant using analysis of variance methods. Using tempera-

ture modulated-DSC, there is evidence that aging increases the blend miscibility as the  $T_{g,PC}$  shifts toward the stationary  $T_{g,ABS}$  during aging. Parallel FTIR investigations found oxidation of butadiene during aging to be even at this relatively low temperature, forming hydroxyl and carbonyl degradation products. The presence of ABS in the blend also appeared to have prevented the shifting from the trans-cis to trans-trans arrangement of the carbonate linkage, which is a well-known phenomenon during elevated temperature aging of PC alone. Moreover, the carbonate linkage appears to have been at the lower energy, trans-trans, arrangement prior to the aging process. © 2008 Wiley Periodicals, Inc. *J Appl Polym Sci* 110: 97–108, 2008

**Key words:** polycarbonate/acrylonitrile–butadiene–styrene blend (PC/ABS); enthalpy relaxation; fictive temperature; Fourier transform infrared (FTIR); differential scanning calorimetry (DSC)

## INTRODUCTION

Polycarbonate/acrylonitrile–butadiene–styrene (PC/ABS) is an amorphous resin blend that is widely used for fabricating thin-walled plastic housings for communication and electronic devices. The blend has been replacing PC over the past decade because it offers properties that merge the favorable properties of its two main constituents. By combining the toughness and higher heat resistance of PC with the flexibility of ABS, PC/ABS blends have higher stiffness over conventional high impact PC or ABS alone, and are easier to process than PC.

Although the use of PC/ABS blends for thin-walled moldings have increased dramatically, the structural recovery behavior of these materials is not as well studied as the main blend constituent, PC. Structural recovery in glassy polymers can cause profound changes in polymer physical and mechani-

cal properties.<sup>1</sup> This phenomenon was first referred to as physical aging by Struik<sup>2</sup> and, unlike chemical aging, is reversible. Physical aging rate is a function of storage (aging) time and temperature below the polymer glass transition. To characterize the physical aging process, the material is allowed to evolve toward equilibrium isothermally without the influence of external conditions.<sup>1</sup> To date, various characterization methods have been used<sup>3–9</sup> to study physical aging in PC material but one of the more accessible techniques is differential scanning calorimetry (DSC),<sup>10–17</sup> which can indirectly measure changes in enthalpy—one of two (the other being volume) bulk thermodynamic properties associated with structural recovery.

To the best of the authors' knowledge, no data on relaxation of PC/ABS other than those by Rusch in 1968<sup>18</sup> are available in the open literature. Patty et al.<sup>19</sup> compared the thermal and moisture stability of PC/ABS with materials traditionally used for automotive instrument panels and found them to be comparable. In some cases, the blend showed improved performance in aging studies, tensile tests, and retention of impact strength. Guest and Van Daele<sup>20</sup> also found that PC/ABS better retained high-impact performance following aging at elevated

Correspondence to: P. Lee-Sullivan (pearls@uwaterloo.ca).

Contract grant sponsor: Ontario Centers of Excellence (OCE) Collaborative Research Program.

Contract grant sponsor: Research in Motion (RIM), Waterloo, Ontario.

temperatures, as compared to PC itself. Further studies of the mechanical properties of PC/ABS have also been reported elsewhere.<sup>21–27</sup>

Recent reports of physical aging studies of blends using DSC techniques can be readily found in the open literature,<sup>28–32</sup> but there does not seem to be any published work on the PC/ABS blend. Moreover, the use of Fourier transform infrared (FTIR) spectroscopy appears to be commonplace for investigating thermal treatments of PC<sup>33–36</sup> and ABS<sup>37–39</sup> polymers. Again, data for the PC/ABS blend are not readily available.

The purpose of this work is to observe, using DSC and FTIR studies, the physical aging behavior of a widely used PC/ABS blend at a temperature below the glass transition of the ABS ( $T_{g,ABS}$ ) component. The selected aging temperature at 80°C is  $\sim 10^\circ\text{C}$  below the lower of the two blend component's glass temperature. The selection was based on a comprehensive set of tests over the range of the two glass transitions which showed that the relaxation response at higher than 80°C will be too fast; this could potentially result in experiments missing important parts of blend relaxation behavior.<sup>40</sup> Following DSC techniques used for PC, the effects of progressive aging on enthalpic relaxation, fictive temperature, and glass transition temperature have been determined. These measurements will supplement the extensive body of literature on aging of PC. The work is particularly interested in investigating, using FTIR techniques, whether the known changes in chemical bonds observed in the individual PC and ABS components during the physical aging process continue on even when the two components are blended. The statistical significance of the changes in some of these measured parameters has been analyzed using analysis of variance (ANOVA).

## EXPERIMENTAL

### Material and specimen preparation

This study investigated a 75 : 25 PC/ABS blend commercially known as Cyclooy C6600. It is a widely used PC/ABS ratio produced by GE Plastics (Bellingham, MA) with a melt flow rate of 21.5 g/10 min at 260°C with 2.16 kg<sub>f</sub> in accordance to the ASTM standard.<sup>41</sup> The weight average molecular weight ( $M_w$ ) of the blend was found to be 45,000 by Jordi FLP using gel permeation chromatography with RI (GPC-RI) and GPC-FTIR techniques. The size of the molecules in solution was found to be the same and could not be resolved using GPC. Moreover, GPC-FTIR confirmed that they were eluting at the same time.

The DMA sample consists of a rectangular bar having dimensions 27.0 × 12.3 × 1.52 mm<sup>3</sup> cut from

a injection-molded plaque. Molding conditions include mixing barrel temperature, 260°C; mold temperature, 80°C; and packing pressure, 1160 kg/cm<sup>2</sup>. For DSC work, a piece of resin between 10 and 12 mg is encapsulated within aluminum hermetic pans. All aging was performed in a VWR Signature 1430M vacuum oven. Thicker sheets of the same material were also prepared using the same molding conditions as mentioned earlier, and test bars with nominal dimensions of 76.2 × 25.4 × 2.84 mm<sup>3</sup> were cut for FTIR studies. Cut edges were gently polished.

### Dynamic mechanical analysis

To facilitate the identification of glass transitions for this blend before conducting DSC work, dynamic mechanical analysis (DMA) was performed to screen the main transitions above room temperature. DMA was performed on a TA Instruments DMA model 2980. The sample bar was mounted onto a single cantilever mode clamp and oscillated at 1 Hz frequency and at a heating rate of 1°C/min.

### Differential scanning calorimetry

Resin samples used for physical aging are studied in a TA Instruments DSC model 2920 used with a refrigeration cooling system attached to provide controlled cooling. Baseline calibrations were also performed daily. Indium is used to perform the temperature and heat flow rate calibration, while sapphire is used for the heat capacity calibration. The indium calibration is performed to ensure a proper melting point value of 156.6°C,<sup>42,43</sup> and a standard heat of fusion of 28.7 J/g<sup>43</sup> is used to obtain the cell constant. The results of the heat capacity calibration are compared to the reported sapphire specific heat capacity<sup>44</sup> for the temperature range of interest for this study. Modulated DSC (MDSC) parameters were selected based on recommendations from TA Instruments technical reports<sup>45–46</sup> and further refined. All MDSC experiments were conducted with an oscillation amplitude of 1°C, period of 70 s, and an underlying heating rate of 1°C/min.

### Analysis of enthalpy relaxation

Since the structural recovery process is completely reversible, all experimental characterization of physical aging must begin by erasing the sample's thermal history. As shown in Figure 1, this is achieved by heating up the sample past its glass transition range and isothermally holding at point *c* for 5–10 min. The erased sample is referred to as the reference. After erasing the thermal history, a three-step thermal treatment is followed: (i) controlled cooling at rate  $q_1$  from the glass transition to the aging tem-

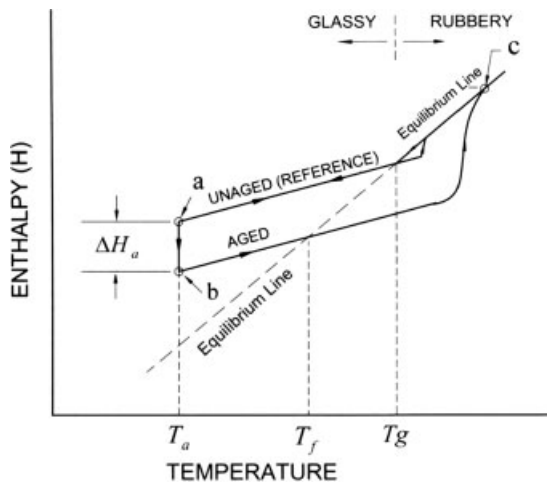


**Figure 1** Schematic of enthalpy evolution during the thermal aging treatment.

perature,  $T_a$ , i.e., from point  $c$  to  $a$ ; (ii) the physical aging treatment itself for a specified time,  $t_a$ , to recover  $\Delta H_a$  enthalpy and finally; (iii) reheating at a controlled rate  $q_2$  from point  $b$  to above glass temperature where it is again in equilibrium. This final heating step will produce an observable endothermic peak at the glass transition region. The peak of the endothermic overshoot occurrence,  $T_p$ , is a function of three experimental parameters,  $q_1$ ,  $\Delta H_a$  and  $q_2$ . Since the intent is to observe aging effects by measuring the peak endotherm, the cooling and heating rates are held constant and identical,  $q_1 = q_2 = 10^\circ\text{C}/\text{min}$ . The enthalpy recovery is thus dictated by the aging temperature and aging time.

In this work, all samples were thermally erased at  $135^\circ\text{C}$  and then aged in an oven at only one aging temperature,  $T_a = 80^\circ\text{C}$ , which is the practical service temperature limit. In total, six aging times,  $t_a = 0.5, 2, 8, 96, 336,$  and  $1008$  h were monitored and for each aging time there were four replicates. In testing each replicate, the aged and the reference (unaged) scans with thermal history erased were recorded. For samples that are aged for longer than 8 h, aging was performed in an oven and then transferred to the DSC in a metal cylinder maintained at the same aging temperature.

The enthalpy recovered on aging,  $\Delta H_a$ , is found simply from the difference in the area under the heat capacity curve during the heat-up of the aged and reference scan. The area can mathematically be expressed using an integral to be evaluated between the aging temperature,  $T_a$ , and a temperature,  $T_c$ , above the glass temperature at which both attain equilibrium.

$$\Delta H_a = \int_{T_a}^{T_c} (C_p)_{\text{aged}} dT - \int_{T_a}^{T_c} (C_p)_{\text{ref}} dT \quad (1)$$

In standard DSC, the total heat flow curves can be converted to heat capacity,  $C_p$  curves, by dividing

the heat flow per unit mass by the instantaneous underlying heating rate.

#### Analysis of MDSC data

Another approach to obtaining DSC data is to modulate the applied temperature. Known as MDSC, the heat flow signals can be conveniently separated as

$$\frac{dH}{dt} = C_p \frac{dT}{dt} + f(T, t) \quad (2)$$

where  $\frac{dH}{dt}$  is the total heat flow rate due to the underlying linear heating rate, and is equivalent to the standard DSC heat flow obtained at the same overall heating rate. This total heat flow can be separated into a heat capacity and melting component,  $C_p \frac{dT}{dt}$ , and a kinetic or time-dependent component,  $f(T, t)$ . The heat capacity component, found as the response to the modulated heating rate, is known as the reversing heat flow signal, and the kinetic component is taken as the difference from the total heat flow and heat capacity component, and is termed the nonreversing heat flow signal. Detailed mathematical expressions for the MDSC technique can be found elsewhere.<sup>47</sup> One benefit of scanning in MDSC mode is that, since enthalpic recovery is a kinetic process, it can be captured in the nonreversing heat flow signal. It is therefore convenient to isolate and integrate the peak in this signal to measure differences in energy content due to aging. This advantage of using the MDSC technique allows one to associate the enthalpy relaxation of a sample simply by determining the area under the nonreversing heat flow curve, but there have been reports<sup>16,48–50</sup> that this was an unreliable method of obtaining the enthalpy relaxation. Accordingly, the conventional DSC method that evaluates the difference in areas of the total heat capacity of aged and unaged samples has been used in this work. The heat capacity derived from the total heat flow is used for quantitative analysis of enthalpy and endothermic peak temperatures, while the reversing heat flow component is employed for qualitative comparisons.

#### Analysis of fictive temperature

Tool<sup>51,52</sup> was the first to develop the fictive temperature,  $T_f$ , a rather useful parameter for defining the structure of a glass based on its previous thermal history. As such,  $T_f$  will vary depending on the rate of cooling, reheating, thermal aging time or temperature or any parameter that affects the previous thermal history of the polymer. The fictive temperature,  $T_f$ , can be determined from the equal area method, as described elsewhere.<sup>17,53</sup> A schematic of the fictive temperature concept that combines the proposals by

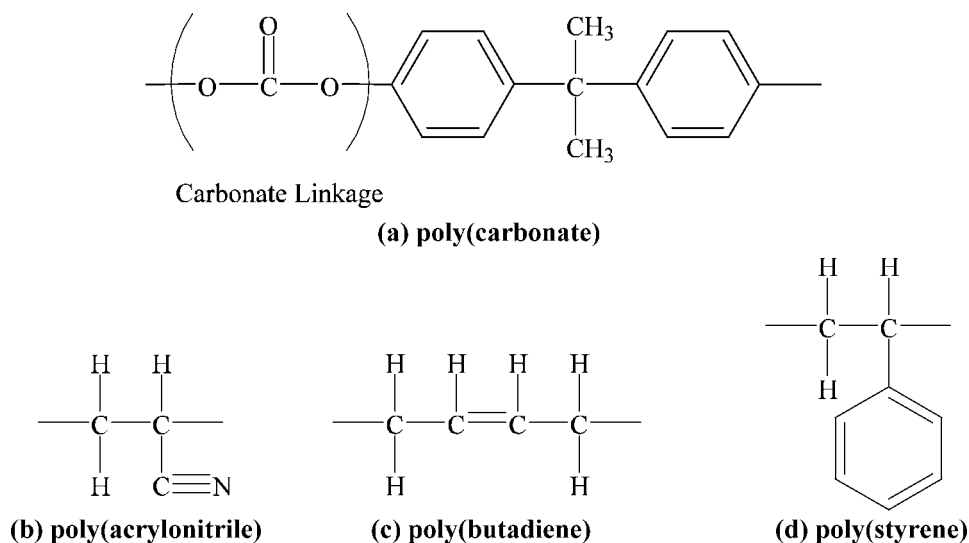


**Figure 2** Molecular structure of (a) polycarbonate, (b) polyacrylonitrile, (c) polybutadiene, and (d) polystyrene.

Refs. 17, 53, and 54 is illustrated in Figure 1. The structural relaxation process occurs during isothermal aging at the aging temperature,  $T_a$ . As the aging process progresses, point  $b$  shifts vertically toward the equilibrium line. Upon reheating, the temperature at which the equilibrium line is reached is defined as the fictive temperature,  $T_f$ . In the case where there is no recovery or aging process, the temperature measured from the equal area method is comparable to the glass temperature.<sup>50</sup>

### FTIR analysis

FTIR spectra were obtained by ATR analysis using a Bruker Optics Tensor27 FTIR attached to a Hyperion microscope with an ATR-II 20 $\times$  objective. The objective consisted of a germanium tip,  $\sim 100\ \mu\text{m}$  in diameter. The molecular structures of the mer groups of the constituent materials in PC/ABS are illustrated in Figure 2. Of particular interest from the spectrum are the C=O stretching of the carbonyl group near  $1770\ \text{cm}^{-1}$ , which corresponds to the bond in the carbonate linkage of PC and the butadiene region near  $960\ \text{cm}^{-1}$ . In these tests, FTIR data were averaged over 100 scans, obtained at a resolution of  $2\ \text{cm}^{-1}$ , from  $700$  to  $4000\ \text{cm}^{-1}$ .

Bar samples cut from the molded sheets were stood on end in grooves machined into an aluminum block. This allowed both surfaces of the sample to be equally exposed to the environment. FTIR spectra were obtained on these samples after 1, 3, 7, and 10 days, and then once every week thereafter for  $\sim 80$  days. The results were replicated with two samples for each spectrum, and these samples that are removed from the oven for FTIR were not reused.

### Statistical analysis of data

It was unclear at the outset if the measured changes during the aging of PC/ABS would be significant since the aging temperature was relatively lower than temperatures normally used in PC studies. To evaluate the statistical significance of changes due to aging over a 1000-h period, the ANOVA method was applied, following a previous approach.<sup>55</sup> Experiments were planned so that sufficient data can be collected and analyzed by statistical methods. The physical aging study is one with a single factor: aging time,  $t_a$ , with six levels of the factor. The analysis of a single-factor with  $a$  levels of the factor (or treatments) is suitably analyzed by a one-way ANOVA experiment. Further details of ANOVA and more in-depth comparisons used in the analysis of this study can be found elsewhere.<sup>56</sup>

## RESULTS AND DISCUSSION

### Glass transition identified by DMA

The DMA profiles shown in Figure 3(a) identifies two glass transition temperatures for both the loss modulus,  $E''$ <sup>57</sup> or the  $\tan \delta$ <sup>58</sup> peak scans. Based on the  $E''$  profile, a large glass transition peak is apparent at  $\sim 112^\circ\text{C}$  but is accompanied by a small shoulder. Using mathematical software, the peak was mathematically deconvoluted, which revealed a second peak occurring near  $100^\circ\text{C}$ , Figure 3(b). The screening results showed that there are indeed two glass transition peaks and that the temperature limits for DSC experiments would be between  $80$  and  $120^\circ\text{C}$ .

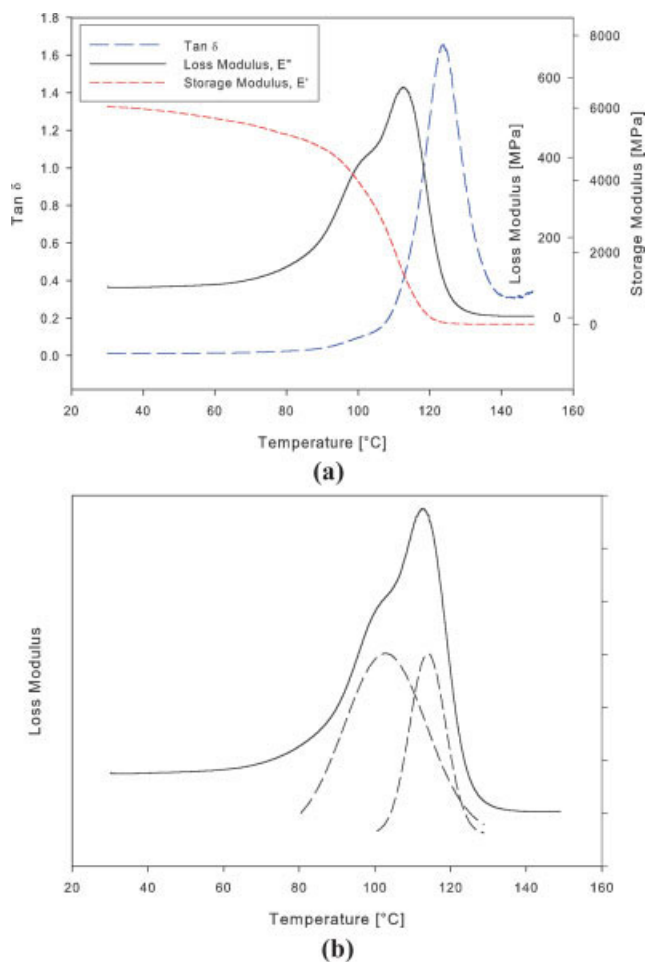


**Figure 3** DMA response on heat-up of PC/ABS as-received material in single cantilever mode: (a) tan  $\delta$ , loss and storage modulus and (b) deconvolution of loss modulus. [Color figure can be viewed in the online issue, which is available at [www.interscience.wiley.com](http://www.interscience.wiley.com).]

### MDSC data

The heat capacity of the sample as a function of temperature is found by dividing the total heat flow by the heating rate of 1°C/min. Figure 4 shows a typical overlay of the total heat capacity curves obtained from heat flow scans during heat-up, which were used to study the peak temperature and enthalpic change after aging at 80°C. At first glance, the endothermic ABS and PC peaks appear to increase in magnitude with increase in aging times. Less obvious, however, is that the endothermic peak temperature for PC actually decreases first before steadily increasing with the aging time. This initial drop has also been noted elsewhere, for example with PVAc.<sup>59</sup> The variations in peak endothermic temperatures for PC and ABS are shown ( $T_p$  versus  $\log |t_a|$ ) in Figure 5.

To analyze enthalpic recovery due to aging at 80°C,  $\Delta H_a$  is evaluated from the difference in the

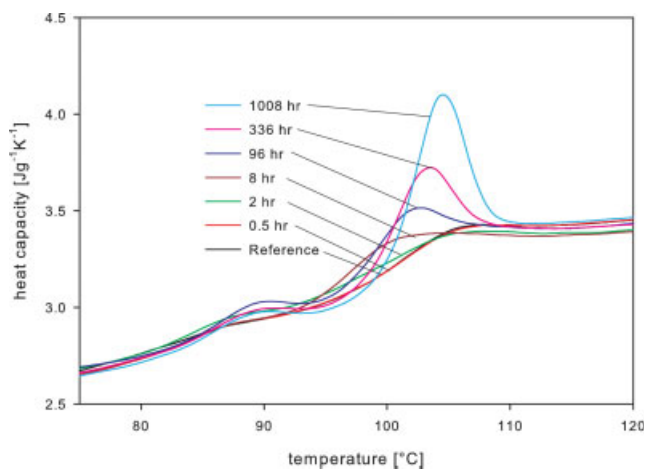


**Figure 4** Overlay of heat capacity curves after aging at 80°C for various aging times. [Color figure can be viewed in the online issue, which is available at [www.interscience.wiley.com](http://www.interscience.wiley.com).]

area under the aged and reference heat capacity curve, and the values for the aging times studied are tabulated in Table I. When  $\Delta H_a$  is plotted against  $\log |t_a|$  in Figure 6, the expected linear relationship of enthalpy recovered,  $\Delta H_{ar}$ , with aging time is seen. Interestingly, however, the slope of the line or rate of change of  $\left(\frac{\partial \Delta H_a}{\partial \log |t_a|}\right)_{q_1, T_a, q_2}$  for the 75 : 25 PC/ABS blend is found to be 0.62 J/g per decade, which is almost identical to PC aged at a much higher temperature of 120°C.<sup>1,11</sup>

When Figures 5 and 6 are viewed together, they suggest that aging has a negligible effect on the ABS component's peak, even though the aging temperature is closer to the glass transition of ABS. It is clear that there is almost no change in the ABS endothermic peak but the PC aging peaks tend to decrease

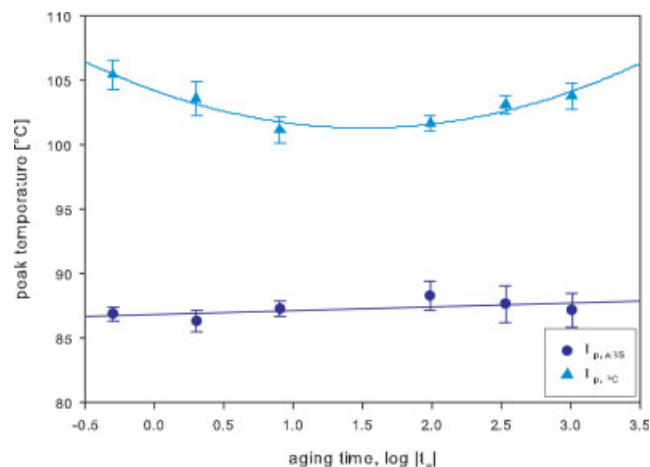


**Figure 5** Dependence of peak endothermic temperature on aging time from heat capacity. [Color figure can be viewed in the online issue, which is available at [www.interscience.wiley.com](http://www.interscience.wiley.com).]

**TABLE I**  
Summary of Enthalpy Recovery Measurements for Samples Aged at 80°C

Aging time, $t_a$ (h)	Area under curve (J/g)		Enthalpy recovered (J/g)	Average (J/g)	Std. dev. (J/g)	RSD (%)
	Aged	Reference				
0.5	1.85	1.61	0.24	0.24	0.012	5.05
	1.93	1.70	0.23			
	1.87	1.62	0.25			
	1.92	1.69	0.22			
2	1.98	1.55	0.43	0.44	0.032	7.26
	2.12	1.65	0.47			
	2.13	1.73	0.40			
	2.20	1.74	0.46			
8	2.21	1.46	0.75	0.72	0.070	9.62
	2.34	1.71	0.63			
	2.31	1.58	0.73			
	2.22	1.43	0.79			
96	2.92	1.60	1.32	1.44	0.086	5.97
	2.98	1.52	1.46			
	2.94	1.41	1.53			
	2.86	1.43	1.43			
336	3.70	1.71	1.99	1.83	0.16	8.53
	3.44	1.68	1.76			
	3.41	1.50	1.91			
	3.08	1.44	1.64			
1008	4.40	1.69	2.71	2.27	0.33	>14.50
	3.72	1.73	1.99			
	3.42	1.36	2.06			
	4.15	1.84	2.31			

before increasing again, which is quite different from previously observed behavior.<sup>11,12</sup> This may be explained by the difference in aged states. The PC blend constituent has similar behavior to a poorly aged PC when aging at 80°C, while reported relationships in Refs. 11 and 12 are single PC polymers aged at much higher temperatures, e.g., 120°C.

A plausible explanation for the difference is that physical aging could have affected the miscibility of the blend, as observed by the convergence of two glass temperatures into one.<sup>28</sup> It would, therefore, not be surprising that, with increasing aging time, the individual endotherms of PC and ABS would also behave in the same way. Figure 5 suggests that aging may have influenced the miscibility of the blend as the peak temperature for PC converges toward that of ABS, but diverges again. One way to gain more insight into this is to analyze the MDSC signals.

If the heat flow scans are deconvoluted into the reversing and nonreversing signals, as described in eq. (2), it is possible to observe the shift in the temperature peaks of the endotherm for PC by comparing the reversing signal. As described elsewhere,<sup>47</sup> the convenience of the MDSC reversing signal permits a convenient qualitative analysis of the polymer's glass temperature. When the reversing heat flow for all the aging times are overlaid in Figure 7(a), the PC transition inflection temperature appears to

decrease with aging time. This is more evident when the derivative of the curves are plotted in Figure 7(b), while Figure 8 illustrates the changes of the glass temperature of the two components in the blend.

These results are consistent with the boiling water aging experiments by Li et al.,<sup>22</sup> in which the results indicated little to no change in the ABS transition temperature in the PC/ABS blend, whereas the PC transition temperature decreased with aging. They,

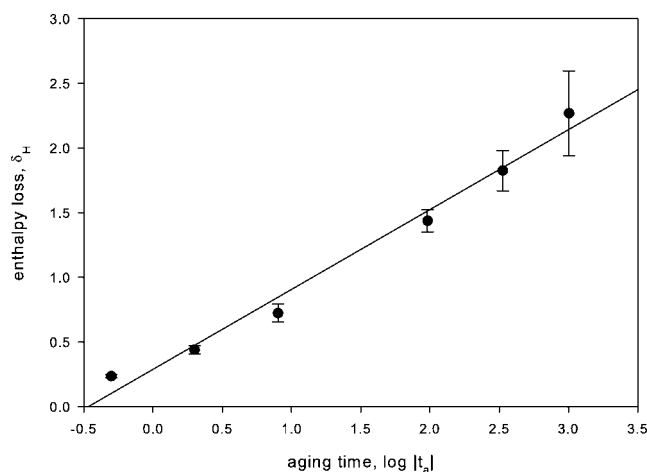


**Figure 6** Dependence of enthalpy loss on aging time (hours).

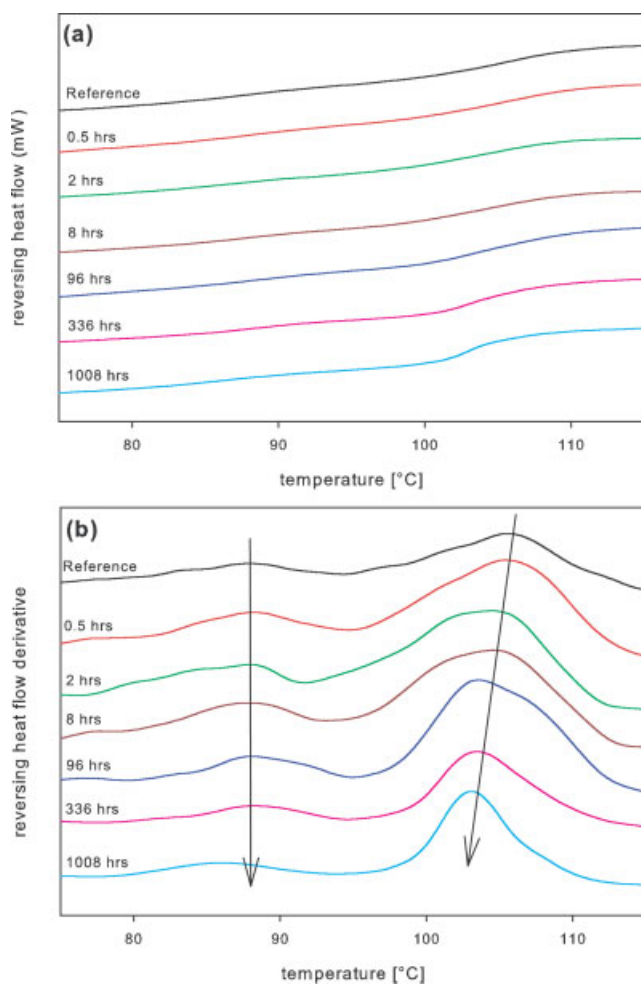


**Figure 7** (a) Reversing heat flow curves after aging at 80°C for different aging times; (b) derivative of reversing heat flow curves in (a). [Color figure can be viewed in the online issue, which is available at [www.interscience.wiley.com](http://www.interscience.wiley.com).]

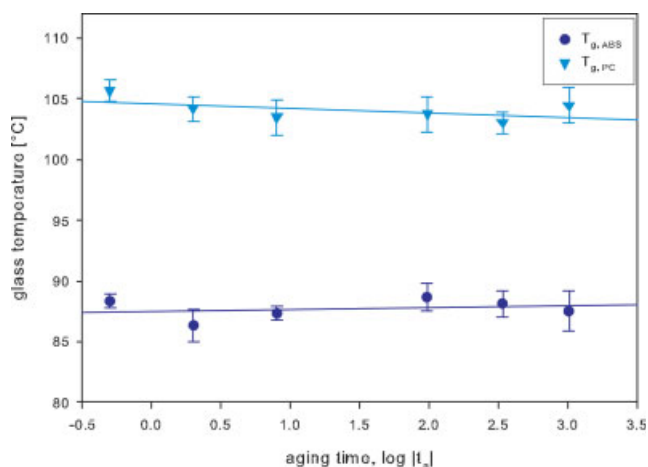


**Figure 8** Dependence of glass temperature on aging time (hours). [Color figure can be viewed in the online issue, which is available at [www.interscience.wiley.com](http://www.interscience.wiley.com).]

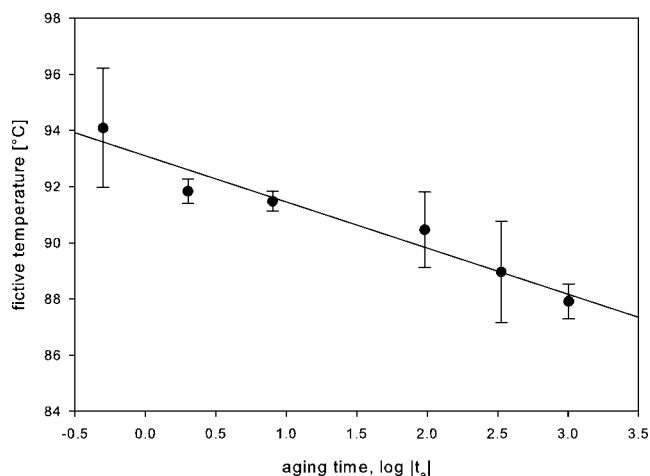


**Figure 9** Dependence of fictive temperature on aging time (hours).

as other researchers,<sup>60–63</sup> have indicated partial miscibility in studies of PC/ABS systems, while others<sup>20,24</sup> have indicated immiscibility. Although two peaks are clearly visible, it has been described by Lodge et al.<sup>64</sup> that

much confusion stems from a naive application of a well known but incorrect rule of thumb, namely, that observation of two distinct glass transitions in a binary polymer blend is a signature of immiscibility. The reason for such confusion is that not only do some miscible systems exhibit two transitions, but any one-phase polymer mixture should be expected to exhibit two distinct transitions if the pure component transitions are sufficiently different.

With the noticeable shift in the inflection of the reversing heat flow, one might be quick to jump to the conclusion that the present PC/ABS blend is partially miscible. However, this is far from certain as a blend's miscibility requires extensive studies by a variety of techniques as proposed by Lodge et al.<sup>64</sup>

Lastly, since the fictive temperature,  $T_f$ , is a more accurate representation of aged state than the glass transition, the effects of aging on the  $T_f$  is plotted in Figure 9. Consistent with enthalpic recover results found in Figure 6,  $T_f$  decreases linearly with  $\log t_a$ , very similar to PC material.<sup>11,65</sup>

#### ATR-FTIR measurements

The results shown in Figure 10(a) of the reference PC/ABS material (e.g., not subjected to any conditioning, only thermal history erased) appear similar to that of the PC component as studied elsewhere.<sup>60</sup> This is somewhat expected, since PC is the main constituent of the blend PC. This spectrum is also visually very similar to that reported by Kuczynski et al.<sup>21</sup> of their PC/ABS blend. For easy comparison,

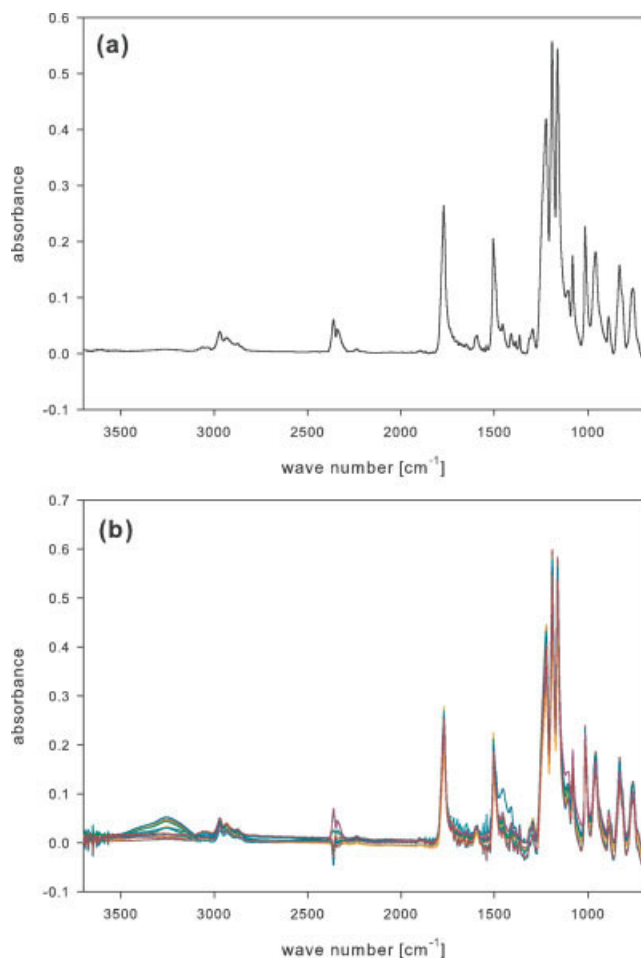


**Figure 10** FTIR spectrum of (a) reference and (b) aged PC/ABS. [Color figure can be viewed in the online issue, which is available at [www.interscience.wiley.com](http://www.interscience.wiley.com).]

the spectra of the samples aged for up to 80 days in this study are overlaid in Figure 10(b).

It has been reported that during oxidation, carbonyl and hydroxyl degradation products are formed and have been monitored in literature.<sup>38,66,67</sup> The study by Motyakin and Schlick<sup>38</sup> on thermal degradation of ABS at high temperatures have monitored the decrease in the butadiene absorption intensity during degradation along with the increase in intensity of the degradation products. A decrease in the absorption intensity of the butadiene region is also seen during the aging process in this study, as shown in Figure 11.

The unaged spectrum shown in Figure 10(a) showed no traces of hydroxyl groups present in the 3000–3500  $\text{cm}^{-1}$  region. However, the spectrum obtained after subsequent aging, Figure 10(b), showed notable increases in the hydroxyl degradation products after 10 days of aging. Upon magnification of the carbonyl ( $\text{C}=\text{O}$ ) region (1770  $\text{cm}^{-1}$ ), it can be seen in Figure 12 that there is indeed an increase in the absorbance intensities over time which supports

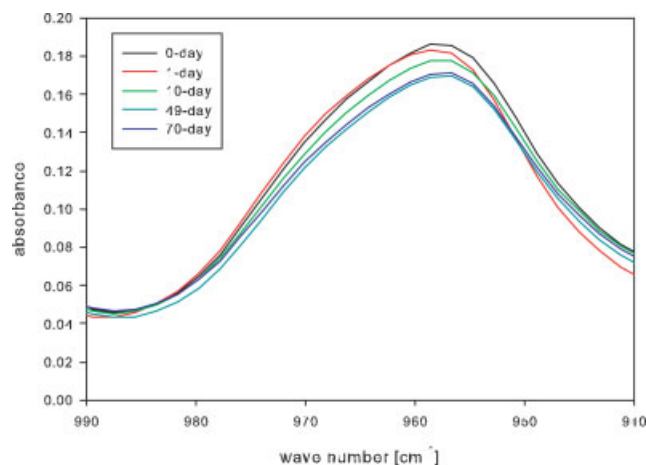


**Figure 11** Absorbance intensity of butadiene region (960  $\text{cm}^{-1}$ ) aged at 80°C. [Color figure can be viewed in the online issue, which is available at [www.interscience.wiley.com](http://www.interscience.wiley.com).]

the oxidation mechanism. Although the degradation products for the oxidation of butadiene are formed, the carbonyl region is also the characteristic group in the carbonate linkage in PC. The  $\text{C}=\text{O}$  bond in the carbonate linkage has a very high dissociation energy as indicated by Li and Huang<sup>68</sup> which makes it suitable for monitoring changes in the spectrum during aging studies.

The peaks of all aged samples at various times are normalized to the height of the reference, unaged, spectrum, and these heights for the butadiene and carbonyl region are plotted in Figure 13. The results show an overall increase of 8% in the intensity of the carbonyl region over the duration of the study, while the butadiene absorbance decreased by  $\sim 8\%$ . The increase in the absorbance intensities of  $\text{C}=\text{O}$

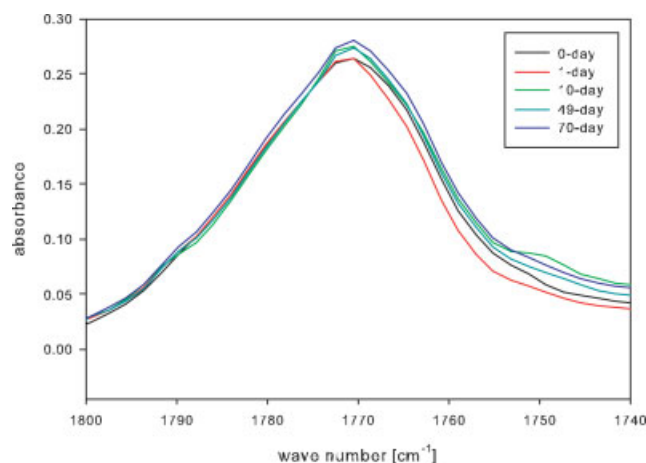


**Figure 12** Absorbance intensity of  $\text{C}=\text{O}$  stretching (1770  $\text{cm}^{-1}$ ) aged at 80°C. [Color figure can be viewed in the online issue, which is available at [www.interscience.wiley.com](http://www.interscience.wiley.com).]



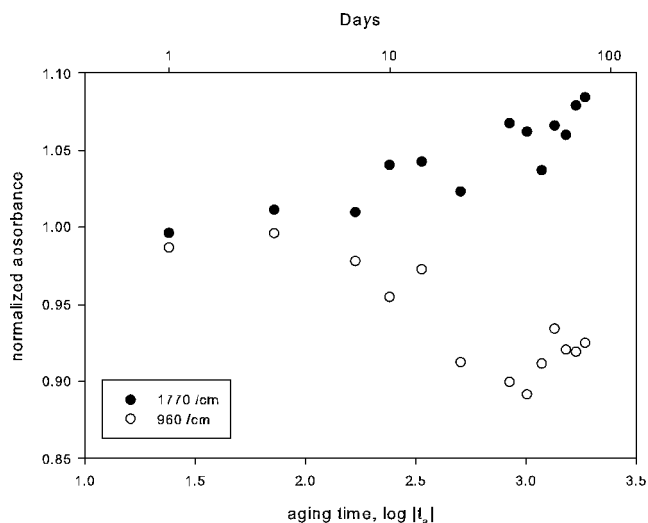


**Figure 13** Normalized peak absorbance intensity of the carbonyl (●) and butadiene (○) region aged at 80°C.

can be attributed to either the degradation of butadiene or with the aging of the PC system as found by Heymans.<sup>36</sup> Figure 13 shows a gradual increase in the carbonyl absorbance at  $\sim 10$  days, while butadiene shows a decrease beginning about the same time. It is also noted that the hydroxyl degradation products form after 10 days of aging. Therefore, it is reasonable to assume that oxidation has occurred, and the oxidation process of butadiene occurs after  $\sim 10$  days to produce the hydroxyl and carbonyl degradation products. However, after the initial drop in the absorption intensity of the butadiene groups, the values remained relatively stable after  $\sim 25$  days. The fact that the absorption intensity reaches a steady value quickly could possibly be linked with the cause of  $T_{g,ABS}$  not shifting during aging, while  $T_{g,PC}$  does. As seen earlier in Figure 6, the enthalpy recovery has yet to achieve equilibrium since the aging temperature is quite low for PC. This is consistent with the absorbance intensities for the carbonyl region not having reached a stable value. It is reasonable to infer that, after the butadiene stabilized, the continued increase in the carbonyl groups is mostly due to the aging of the PC component.

Heymans<sup>36</sup> not only showed that the absorbance intensities for the carbonyl group increased with aging in PC but that the aging process at  $\sim 10^\circ\text{C}$  below  $T_g$  led to modifications of the arrangement in the carbonate group. Schmidt et al.<sup>69</sup> had identified that the C=O stretching contained contributions from trans-trans (t-t) conformers at  $1767\text{ cm}^{-1}$  and trans-cis (t-c) conformers at  $1785\text{ cm}^{-1}$ . The modifications were once again confirmed by Lu et al.,<sup>35</sup> showing conformation changes from high-energy t-c conformation into low-energy t-t conformation gradually upon aging at  $127^\circ\text{C}$ . However, aging at room

temperature did not result in an increase nor shifting of the spectra.<sup>36</sup>

It is quite evident from Figure 12 that the carbonyl peak occurs at  $\sim 1770\text{ cm}^{-1}$ , which is already very close to the low-energy t-t conformation. Moreover, no noticeable shifts were observed during the subsequent aging process. This can be attributed to the presence of the ABS which may be restricting further conformation rearrangements, or more likely, that the PC chain segments already exist in the lower energy state ( $1770\text{ cm}^{-1}$ ).

The ring stretching vibration bands of the phenyl groups (benzene ring) which exist in both the PC and ABS (as part of the styrene component) occurs around  $1600\text{ cm}^{-1}$ . Heymans<sup>34</sup> had first reported conformational changes in PC by the investigation of the C=O stretching in the carbonate linkage, but had since moved on to investigate the potentially cleaner band at  $1600\text{ cm}^{-1}$ , free of Fermi resonance that could obscure changes expected to be seen in physical aging.<sup>36</sup> However, that study was not successful in observing any conformational changes. The contributions from the t-t and t-c conformers can be clearly seen in Figure 14 without deconvolution. The two-peak region of the absorption intensities appears to remain constant throughout the duration of the aging study, and also show no shifting of either t-t or t-c conformational contributions.

Another point of interest is that the characteristic C $\equiv$ N absorption band for the acrylonitrile component occurring near  $2250\text{ cm}^{-1}$  is either in very small undetectable amounts or nonexistent in the blend. This is evident in the full spectrum seen in Figure 10 of our results, as well as in the work of Kuczynski et al.<sup>21</sup>

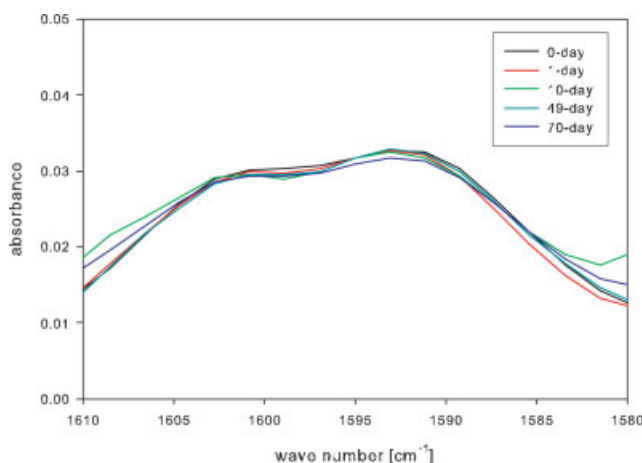


**Figure 14** Absorbance intensity of phenyl group stretching ( $1600\text{ cm}^{-1}$ ) aged at  $80^\circ\text{C}$ . [Color figure can be viewed in the online issue, which is available at [www.interscience.wiley.com](http://www.interscience.wiley.com).]

**TABLE II**  
ANOVA Results for PC-ABS Aging Study

Source	Variable	Sums of squares	Degrees of freedom	Mean square	<i>P</i> -value
$t_a$	$T_{p,ABS}$	7.61	5	1.52	0.265
	$T_{p,PC}$	36.22	5	7.24	0.001
	$T_{g,ABS}$	14.19	5	2.84	0.092
	$T_{g,PC}$	18.31	5	3.66	0.025
Error	$T_{p,ABS}$	19.31	18	1.07	
	$T_{p,PC}$	19.30	18	1.07	
	$T_{g,ABS}$	22.60	18	1.26	
	$T_{g,PC}$	19.54	18	1.09	
Total	$T_{p,ABS}$	26.92	23		
	$T_{p,PC}$	55.52	23		
	$T_{g,ABS}$	36.79	23		
	$T_{g,PC}$	37.84	23		

### Analysis of variance

The statistical analysis technique, ANOVA, was applied to analyze the peak endothermic data to verify whether the changes in the selected DSC data with increasing aging time,  $t_a$ , are indeed significant. These changes include the enthalpic peak temperature,  $T_p$ , for each component in the blend, and the shifts in the two glass transitions. Experimental data have been validated before performing ANOVA analysis, and the details of this validation process can be found in Ref. 56.

The sums of squares is a measure of variability.<sup>56</sup> It can be seen from Table II that the treatment,  $t_a$ , as compared to the error, accounts for a large amount of the total variability for  $T_{p,PC}$ , which is favorable. This means that the differences in the observations are accounted for by the applied treatment, as opposed to random errors,  $\epsilon$ . In contrast, there is greater uncertainty for  $T_{p,ABS}$  and hence much weaker significance ( $P = 0.265$ ) as compared to  $T_{p,PC}$  ( $P = 0.001$ ). Differences found in  $T_{p,ABS}$ , however, may not be a direct result of the aging time, but perhaps due to variability caused by random error. The statistically insignificant differences between the peak endothermic temperatures for ABS are consistent with Figure 5. On the other hand, the strong significance of  $T_{p,PC}$  concludes that its null hypothesis can be rejected. Although it is understood that there are notable differences among the different treatments (different aging times) for  $T_{p,PC}$ , it is unclear which pair of comparisons has caused the significant statistical differences. From the statistical Tukey's multiple comparisons shown in Table III for  $T_{p,PC}$ , each level of treatment is compared directly to all other levels of the treatment. Those that yield significant statistical differences ( $P \leq 0.05$ ) are marked with an asterisk.

From the results of the multiple comparisons from Table III and polynomial contrasts in Table IV, it is suggested that  $T_{p,PC}$  follows a parabolic shape. Table IV

**TABLE III**  
Tukey's Multiple Comparisons for Peak Endothermic Temperature of PC Component

$t_a$ (i)	$t_a$ (j)	<i>P</i> -value
0.5	2.0	0.057
	8.0	0.001*
	96.0	0.006*
	336.0	0.192
2.0	1008.0	0.783
	0.5	0.057
	8.0	0.455
	96.0	0.883
8.0	336.0	0.984
	1008.0	0.480
	0.5	0.001*
	2.0	0.455
96.0	96.0	0.967
	336.0	0.168
	1008.0	0.018*
	0.5	0.006*
336.0	2.0	0.883
	8.0	0.967
	336.0	0.522
	1008.0	0.086
1008.0	0.5	0.192
	2.0	0.984
	8.0	0.168
	96.0	0.522
	1008.0	0.854
	0.5	0.783
	2.0	0.480
	8.0	0.018*
	96.0	0.086
	336.0	0.854

\* Observed difference is significant at a 0.05 level.

indicates that  $T_{p,PC}$  results are significant to a second-order least-squares ( $P = 0.00$ ) fit and not at other (higher) orders, whereas it has been found in literature that the peak endothermic temperature for PC increases linearly (first order) with aging time.<sup>12</sup>  $T_{p,ABS}$  was found to be significant at a third-order polynomial fit. However, with a small data set (six treatments), it is not possible to confidently assume that higher orders (third-order) would apply.

From the ANOVA in Table III, the *P*-value of 0.09 for the glass temperatures of the ABS component is at the margin of statistical significance. Because of this, it becomes a judgemental decision on the part of the researcher whether this is of practical value

**TABLE IV**  
Polynomial Contrasts of Peak Endothermic Temperature for PC Component

Polynomial contrast	<i>P</i> -value
Linear	0.539
Quadratic	0.000
Cubic	0.150
Order 4	0.441
Order 5	0.779

and this uncertainty, as depicted by the relatively flat linear fit in the figure, is also reflected in the  $P$ -value from ANOVA which indicates near significance. Prior to the statistical analysis, it was observed in Figure 8 that there was a subtle decrease in the PC component glass temperature, as was found in literature as well.<sup>26</sup> The observed decrease is confirmed with  $P = 0.025$  for  $T_{g,PC}$  indicating statistical significance in the observed data.

### CONCLUDING REMARKS

The enthalpic relaxation rate for the investigated 75 : 25 PC/ABS blend aged at 80°C is 0.62 J/g per decade of aging time. The rate is very similar to the reported values for polycarbonate aged at ~ 120°C. Using ANOVA, it was verified that the changes in the PC endothermic peak temperature are indeed significant. The peak endothermic temperature for ABS is, however, insensitive to aging. This was unexpected since the aging temperature is only 10°C below the  $T_{g,ABS}$  but 30°C below  $T_{g,PC}$ . Modulated temperature DSC data strongly suggest that the blend miscibility changes with aging but this remains to be confirmed.

In a parallel study using FTIR, it was found that oxidation occurred in butadiene, creating carbonyl and hydroxyl groups degradation products. The expected change of the carbonate conformation in PC from trans-cis to trans-trans during aging was not detectable in the PC/ABS blend, possibly due to the presence of ABS.

The authors gratefully acknowledge the assistance of RIM project collaborators, Dr. Dwayne Wasylshyn and Dr. Bev Christian, who provided all samples and technical coordination support to Mr. Jacky Tang.

### References

- Hutchinson, J. M. *Prog Polym Sci* 1995, 20, 703.
- Struik, L. C. E. *Physical Aging in Amorphous Polymers and Other Materials*; Elsevier: Amsterdam, 1978.
- Málek, J.; Shanelova, J. *J Therm Anal Calorim* 2000, 60, 975.
- Málek, J. *Thermochim Acta* 1998, 313, 181.
- Málek, J.; Montserrat, S. *Thermochim Acta* 1998, 313, 191.
- Lu, J.; Wang, Y.; Shen, D. *Polym Prepr* 2000, 41, 1167.
- Schultheisz, C. R.; McKenna, G. B. *Polym Mater Sci Eng Proc ACS Div PMSE* 1997, 76, 221.
- Cheng, T. W.; Keskkula, H.; Paul, D. R. *J Appl Polym Sci* 1992, 45, 531.
- Liu, L. B.; Yee, A. F.; Gidley, D. W. *J Polym Sci: Part B: Polym Phys* 1992, 30, 221.
- Hadac, J.; Slobodian, P.; Saha, P. *J Therm Anal Calorim* 2005, 80, 181.
- Lee-Sullivan, P.; Bettle, M. *J Therm Anal Calorim* 2005, 81, 169.
- Hutchinson, J. M.; Smith, S.; Horne, B.; Gourlay, G. M. *Macromolecules* 1999, 32, 5046.
- Hodge, I. M. *Macromolecules* 1983, 16, 898.
- Bauwens-Crowet, C.; Bauwens, J. C. *Polymer* 1986, 27, 709.
- Rault, J. *J Phys Condens Matter* 2003, 15, S1193.
- Hutchinson, J. M.; Tong, A. B.; Jiang, Z. *Thermochim Acta* 1999, 335, 27.
- Moynihan, C. T.; Easteal, A. J.; DeBolt, M. A.; Tucker, J. *J Am Ceram Soc* 1976, 59, 12.
- Rusch, K. C. *J Macromol Sci Phys* 1968, B2, 421.
- Patty, B. S.; Ceraso, J.; Novak, L.; Pham, H. T. *Annu Techn Conf ANTEC Conf Proc* 2004, 3, 4054.
- Guest, M. J.; Van Daele, R. *J Appl Polym Sci* 1995, 55, 1417.
- Kuczynski, J.; Snyder, R. W.; Padolak, P. P. *Polym Degrad Stab* 1994, 43, 285.
- Li, C.; Zhang, Y.; Zhang, Y. *J Appl Polym Sci* 2003, 89, 589.
- Nichols, K.; Doonan, T.; Maher, J. In *Annu Technical Conference ANTEC Conference Proceedings*, 1991; p 800.
- Más, J.; Vidaurre, A.; Meseguer, J. M.; Romero, F.; Monleon Pradas, M.; Gomez Ribelles, J. L.; MasPOCH, M. L. L.; Santana, O. O.; Pages, P.; Perez-Folch, J. *J Appl Polym Sci* 2002, 83, 1507.
- Wang, C. H. *Annu Techn Conf ANTEC Conf Proc* 1995, 2, 1946.
- Eguiazabal, J. I.; Nazabal, J. *J Polym Eng Sci* 1990, 30, 527.
- Khan, M. M. K.; Liang, R. F.; Gupta, R. K.; Agarwal, S. *Korea Australia Rheol J* 2005, 17, 1.
- Su, C. C.; Shih, C. K. *J Appl Polym Sci* 2006, 100, 3840.
- Arrighi, V.; Cowie, J. M. G.; Ferguson, R.; McEwen, I. J.; McGonigle, E.; Pethrick, R. A.; Princi, E. *Polym Int* 2005, 55, 749.
- Lee, J. K.; Im, J. E.; Park, J. H.; Won, H. Y.; Lee, K. H. *J Appl Polym Sci* 2006, 99, 2220.
- Aouachria, K.; Belhaneche-Bensemra, N. *Polym Test* 2006, 25, 1101.
- Zheng, S.; Kangming, N.; Qipeng, G. *Thermochim Acta* 2004, 419, 267.
- Jang, B. N.; Wilkie, C. A. *Thermochim Acta* 2005, 426, 73.
- Heymans, N. *Polymer* 1997, 38, 3435.
- Lu, J.; Wong, Y.; Shen, D. *Polym J* 2000, 32, 610.
- Heymans, N.; Van Rossum, S. *J Mater Sci* 2002, 37, 4273.
- Botros, S. H.; Moustafa, A. F.; Ibrahim, S. A. *Polym Plast Technol Eng* 2006, 45, 503.
- Motyakin, M. V.; Schlick, S. *Polym Degrad Stab* 2002, 76, 25.
- Suzuki, M.; Wilkie, C. A. *Polym Degrad Stab* 1995, 47, 217.
- Tang, J. *Physical Aging and Hygrothermal Response of Polycarbonate/Acrylonitrile-Butadiene-Styrene Polymer Blend*; MASc Thesis, University of Waterloo; 2007.
- ASTM D 1238. *Standard Test Method for Melt Flow Rates of Thermoplastics by Extrusion Plastometer*; 1991.
- ASTM E 967. *Temperature Calibration of Differential Scanning Calorimeters and Differential Thermal Analyzers*; 2003.
- ASTM E 968. *Heat Flow Calibration of Differential Scanning Calorimeters*; 2002.
- ASTM E 1269. *Standard Test Method for Determining Specific Heat Capacity by Differential Scanning Calorimetry*; 2001.
- Thomas, L. C. *Modulated DSC paper 3: Modulated DSC basics; Optimization of MDSC experimental conditions*; Technical report, TA Instruments, 2005.
- Thomas, L. C. *Modulated DSC paper 5: Measurement of glass transitions and enthalpic recovery*; Technical report, TA Instruments, 2005.
- Thomas, L. C.; *Modulated DSC paper 1: Why modulated DSC? An overview and summary of advantages and disadvantages relative to traditional DSC*; Technical report, TA Instruments, 2005.
- Simon, S. L.; McKenna, G. B. *Thermochim Acta* 2000, 348, 77.
- Simon, S. L. *Thermochim Acta* 2001, 374, 55.
- McKenna, G. B.; Simon, S. L. In *Handbook of Thermal Analysis and Calorimetry, Vol. 3: Applications to Polymers and Plastics*; Cheng, S. Z. D., Ed.; Elsevier: Amsterdam, 2002; Chapter 2, p 49.

51. Tool, A. Q. United States Bureau Standards J Res 1945, 34, 199.
52. Tool, A. Q. Am Ceram Soc J 1946, 29, 240.
53. Richardson, M. J.; Savill, N. G. Polymer 1975, 16, 753.
54. Moynihan, C. T.; Lee, S. K.; Tatsumisago, M.; Minami, T. Thermochim Acta, 1996, 280–281, 153.
55. Dykeman, D.; Lee-Sullivan, P. Polym Eng Sci 2003, 43, 383.
56. Montgomery, D. C. Design and Analysis of Experiments, 5th ed.; Wiley: New York, 2001.
57. Seyler, R. J. STP 1249: Assignment of the Glass Transition; American Society for Testing and Materials (ASTM): Philadelphia, 1994.
58. Ferrillo, R. G.; Achorn, P. J. J Appl Polym Sci 1997, 64, 191.
59. Hutchinson, J. M.; Kumar, P. Thermochim Acta 2002, 391, 197.
60. Balart, R.; Lopez, J.; Garcia, D.; Salvador, M. D. Eur Polym J 2005, 41, 2150.
61. Nigam, I.; Nigam, D.; Mathur, G. N. Polym Plast Technol Eng 2005, 44, 815.
62. Keitz, J. D.; Barlow, J. W.; Paul, D. R. J Appl Polym Sci 1984, 29, 3131.
63. Santana, O. O.; Maspoch, M. L. L.; Martinez, A. B. Polym Bull 1998, 41, 721.
64. Lodge, T. P.; Wood, E. R.; Halley, J. C. J Polym Sci: Part B: Polym Physics 2006, 44, 756.
65. Ho, C. H.; Vu-Khanh, T. Theor Appl Fract Mech 2004, 41, 103.
66. Rjeb, A.; Tajounte, L.; Chafik El Idrissi, M.; Letarte, S.; Adnot, A.; Roy, D.; Claire, Y.; Périchaud, A.; Kaloustian, J. J Appl Polym Sci 2000, 77, 1742.
67. Gugumus, F. Polym Degrad Stab 1998, 62, 235.
68. Li, X. G.; Huang, M. R. Polym Int 1999, 48, 387.
69. Schmidt, P.; Dybal, J.; Turska, E.; Kulczycki, A. Polymer 1991, 32, 1862.